REPORT DOCUMENTATION PAGE

Form Approved
OMB No. 0704-0188

1. REPORT DATE *(DD-MM-YYYY)*	2. REPORT TYPE	3. DATES COVERED *(From - To)*
2004	Open Literature	

4. TITLE AND SUBTITLE
Reduced Acetylcholine Receptor Density, Morphological Remodeling, and Butyrylcholinesterase Activity Can Sustain Muscle Function in Acetylcholinesterase Knockout Mice

5a. CONTRACT NUMBER

5b. GRANT NUMBER

5c. PROGRAM ELEMENT NUMBER

6. AUTHOR(S)
Adler, M., Manley, H.A., Purcell, A.L., Deshpande, S.S., Hamilton, T.A., Kan, R.K., Oyler, G., Lockridge, O., Duysen, E.G., Sheridan, R.E.

5d. PROJECT NUMBER

5e. TASK NUMBER

5f. WORK UNIT NUMBER

7. PERFORMING ORGANIZATION NAME(S) AND ADDRESS(ES)

US Army Medical Research Institute of Chemical Defense
ATTN: MCMR-UV-PN
3100 Ricketts Point Road
Aberdeen Proving Ground, MD 21010-5400

8. PERFORMING ORGANIZATION REPORT NUMBER

USAMRICD-P02-024

9. SPONSORING / MONITORING AGENCY NAME(S) AND ADDRESS(ES)

US Army Medical Research Institute of Institute of Chemical Defense
ATTN: MCMR-UV-RC
3100 Ricketts Point Road
Aberdeen Proving Ground, MD 21010-5400

10. SPONSOR/MONITOR'S ACRONYM(S)

11. SPONSOR/MONITOR'S REPORT NUMBER(S)

12. DISTRIBUTION / AVAILABILITY STATEMENT

Approved for public release; distribution unlimited

13. SUPPLEMENTARY NOTES
Published in Muscle & Nerve, 30, 317-327, 2004.

14. ABSTRACT
See reprint.

15. SUBJECT TERMS
Acetylcholinesterase, knockout mice, muscle function, butyrylcholinesterase

16. SECURITY CLASSIFICATION OF:			17. LIMITATION OF ABSTRACT	18. NUMBER OF PAGES	19a. NAME OF RESPONSIBLE PERSON
a. REPORT	b. ABSTRACT	c. THIS PAGE			Michael Adler
UNCLASSIFIED	UNCLASSIFIED	UNCLASSIFIED	UNLIMITED	11	19b. TELEPHONE NUMBER *(include area code)* 410-436-1913

ABSTRACT: Nerve-evoked contractions were studied in vitro in phrenic nerve–hemidiaphragm preparations from strain 129X1 acetylcholinesterase knockout ($AChE^{-/-}$) mice and their wild-type littermates ($AChE^{+/+}$). The $AChE^{-/-}$ mice fail to express AChE but have normal levels of butyrylcholinesterase (BChE) and can survive into adulthood. Twitch tensions elicited in diaphragms of $AChE^{-/-}$ mice by single supramaximal stimuli had larger amplitudes and slower rise and decay times than did those in wild-type animals. In $AChE^{-/-}$ preparations, repetitive stimulation at frequencies of 20 and 50 Hz and at 200 and 400 Hz produced decremental muscle tensions; however, stimulation at 70 and 100 Hz resulted in little or no loss of tension during trains. Muscles from $AChE^{+/+}$ mice maintained tension at all frequencies examined but exhibited tetanic fade after exposure to the selective AChE inhibitor 1,5-bis(4-allyldimethyl-ammoniumphenyl)pentane-3-one (BW 284C51). The ability of diaphragm muscles from $AChE^{-/-}$ mice to maintain tension at 70 and 100 Hz suggests a partial compensation for impairment of acetylcholine (ACh) hydrolysis. Three mechanisms—including a reliance on BChE activity for termination of ACh action, downregulation of nicotinic acetylcholine receptors (nAChRs), and morphological remodeling of the endplate region—were identified. Studies of neuromuscular transmission in this model system provide an excellent opportunity to evaluate the role of AChE without complications arising from use of inhibitors.
Muscle Nerve **30:** 317–327, 2004

REDUCED ACETYLCHOLINE RECEPTOR DENSITY, MORPHOLOGICAL REMODELING, AND BUTYRYLCHOLINESTERASE ACTIVITY CAN SUSTAIN MUSCLE FUNCTION IN ACETYLCHOLINESTERASE KNOCKOUT MICE

MICHAEL ADLER, PhD,[1] HEATHER A. MANLEY, PhD,[1] ANGELA L. PURCELL, PhD,[1] SHARAD S. DESHPANDE, PhD,[2] TRACEY A. HAMILTON,[3] ROBERT K. KAN, PhD,[3] GEORGE OYLER, MD, PhD,[4] OKSANA LOCKRIDGE, PhD,[5] ELLEN G. DUYSEN,[5] and ROBERT E. SHERIDAN, PhD[1]

[1] Neurotoxicology Branch, Pharmacology Division, US Army Medical Research Institute of Chemical Defense, Aberdeen Proving Ground, Maryland 21010, USA
[2] Battelle Eastern Regional Technology Center, Aberdeen, Maryland, USA
[3] Comparative Pathology Branch, Comparative Medicine Division, US Army Medical Research Institute of Chemical Defense, Aberdeen Proving Ground, Maryland, USA
[4] Department of Neurology, University of Maryland School of Medicine and Veteran's Affairs Medical Center, Baltimore, Maryland, USA
[5] Eppley Institute, Department of Biochemistry and Molecular Biology, University of Nebraska Medical Center, Omaha, Nebraska, USA

Accepted 13 April 2004

The vertebrate neuromuscular junction is designed for rapid transmission of excitatory signals for initiation of muscle contraction.[5] Among the features responsible for the high throughput of this synapse are the close proximity of the presynaptic and postsynaptic membranes,[10] the direct coupling of acetylcholine (ACh) binding to the opening of the ion channel associated with the nicotinic acetylcholine receptor (nAChR),[27] the brief open time of this channel,[21,27] and the presence of cholinesterase (ChE) for hydrolysis of ACh.[21,30] At the endplate, there are two distinct ChEs for transmitter hydrolysis: acetylcholinesterase (EC 3.1.1.7, AChE) and butyrylcholinesterase (EC 3.1.1.8, BChE).[33] Both enzymes can exist in a multisubunit, collagen-tailed form with selective localization at the endplate basal

The opinions or assertions contained herein are the private views of the authors and are not to be construed as official or as reflecting the views of the Army or the Department of Defense.

Abbreviations: ACh, acetylcholine; AChE, acetylcholinesterase; BChE, butyrylcholinesterase; BW 284C51, 1,5-bis(4-allyldimethyl-ammoniumphenyl)pentane-3-one; d-TC, *d*-tubocurarine; EM, electron microscopy; iso-OMPA, tetraisopropylpyrophosphoramide; mAChR, muscarinic acetylcholine receptor; nAChR, nicotinic acetylcholine receptor

Key words: acetylcholine; acetylcholine receptor; acetylcholinesterase; butyrylcholinesterase; diaphragm; knockout mice; muscle tension

Correspondence to: M. Adler; e-mail: Michael.Adler@amedd.army.mil

Published online 22 July 2004 in Wiley InterScience (www.interscience.wiley.com). DOI 10.1002/mus.20099

lamina.[33] Because of its superior catalytic activity for ACh hydrolysis, AChE is the dominant enzyme, whereas the role of BChE is generally evident only after AChE is inhibited.[3,4]

Inhibition of ChE results in a progressive accumulation of ACh, especially during periods of repetitive stimulation, leading to desensitization of nAChRs and consequent muscle weakness.[12,17] Under this condition, transmitter persists beyond its normal lifetime and is slowly removed from the endplate region by diffusion.[21,30] Diffusion is impeded in part by morphological barriers, such as the apposition of the nerve terminal to the postjunctional membrane,[5,10] and by the high density of postjunctional nAChRs.[21,22,25] If ChE is inhibited pharmacologically or removed by collagenase treatment, repeated binding to nAChR makes diffusional loss of ACh slow and inefficient.[21,22,30] The influence of nAChRs on retention of transmitter was termed "buffered diffusion" by Katz and Miledi[21] and accounts for findings that elimination of ACh is considerably slower than that expected for free diffusion.[30]

Inhibitors of ChE are highly toxic, producing incapacitation and death within minutes.[28] The cause of death is complex, involving loss of central respiratory drive,[6,29] bronchospasm,[1,2] and the inability of the diaphragm muscle to sustain tetanic tension.[19] Because most ChE inhibitors show little selectivity between AChE and BChE, and may have direct actions unrelated to ChE inhibition, it is difficult to establish the role of AChE activity in neuromuscular transmission. To overcome this difficulty, we studied twitch and tetanic tensions in diaphragm muscles from AChE knockout ($AChE^{-/-}$) mice that fail to express AChE but do contain normal levels of BChE.[7,24,36] Stimulation of the phrenic nerve in isolated diaphragm preparations from $AChE^{-/-}$ mice revealed large single twitches and sustained tetanic tensions at 70 and 100 Hz. These findings suggest that, over a limited frequency range, diaphragm muscles from $AChE^{-/-}$ mice are able to compensate for the loss of AChE activity. An understanding of these adaptive mechanisms is expected to provide insight on protection strategies that may be effective against the toxic actions of ChE inhibitors such as the highly lethal nerve agents.

MATERIALS AND METHODS

Animals. Experiments were performed on strain 129X1 $AChE^{-/-}$ and $AChE^{+/+}$ mice of either sex (University of Nebraska Medical Center, Omaha, Nebraska). The $AChE^{+/+}$ mice were maintained on mouse chow and water ad libitum and were 53 ± 4 days old at the time of sacrifice; $AChE^{-/-}$ mice were fed a diet of liquid Ensure Fiber, which was required for their survival,[7,13,14] and were 57 ± 5 days old at sacrifice. All other conditions for animal maintenance were identical and conformed to appropriate federal standards and the Association for Assessment and Accreditation of Laboratory Animal Care (AAALAC) regulations. We complied with the regulations and standards of the Animal Welfare Act and adhered to the principles of the Guide for the Care and Use of Laboratory Animals (NRC 1996).

Contractility Measurements. Tension measurements were performed in vitro on phrenic nerve–hemidiaphragm preparations. The animals were killed by decapitation after being rendered unconscious in a CO_2 chamber. Hemidiaphragms with attached phrenic nerves were mounted in tissue baths at 37°C and immersed in an oxygenated physiological solution of the following composition (mM): NaCl, 135; KCl, 5.0; $MgCl_2$, 1.0; $CaCl_2$, 2.0; $NaHCO_3$, 15.0; Na_2HPO_4, 1.0; glucose, 11.0. The solution was bubbled with a gas mixture of 95% O_2 and 5% CO_2 and had a pH of 7.3.

To obtain single twitches, the phrenic nerve was stimulated with 0.2-ms supramaximal pulses. The response of muscles to repetitive stimulation was probed by eliciting 500-ms trains at frequencies of 20, 50, 70, 100, 200, and 400 Hz. To avoid neuromuscular fatigue, trains were elicited at 30-s intervals. An equilibration period of 20 min was allowed for all drug solutions prior to recording. Muscle twitches were measured with isometric force transducers (FORT 10, WP Instruments, Sarasota, Florida) and analyzed using pClamp software (Axon Instruments, Union City, California).

ChE Assays. The AChE and BChE were extracted from diaphragm muscle by homogenizing in 10 vol of ice-cold 50 mM potassium phosphate (pH 7.0) containing 0.5% Tween-20. The homogenate was centrifuged to remove particulates, and the supernatant was assayed for ChE activity by measuring absorbance at 412 nm using 1 mM acetylthiocholine or 1 mM butyrylthiocholine as substrate for AChE or BChE, respectively.[15] The reactions were carried out in 100 mM potassium phosphate (pH 7.0) and 0.5 mM dithiobisnitrobenzoic acid at 25°C. Inhibition of ChE activity by 1 μM tetraisopropylpyrophosphoramide (iso-OMPA) or 1 μM 1,5-bis(4-allyldimethyl-ammoniumphenyl)pentane-3-one (BW 284C51) was examined after preincubating with inhibitor for 30 min.

Fluorescent α-Bungarotoxin Studies. Diaphragm muscles were pinned onto Sylgard-coated dishes, rinsed three times in calcium- and magnesium-free phosphate-buffered saline (PBS, pH 7.4), and fixed for 1 h in PBS containing 2% paraformaldehyde. Following fixation, tissues were incubated in PBS containing 30% sucrose at 4°C for 16 h, washed three times with ice-cold PBS, embedded in OCT medium and cryosectioned at −20°C. Tissue sections (10 μm) were transferred to positively charged glass slides and stored at −45°C with desiccant until use. Prior to staining for nAChRs, nonspecific binding sites were blocked with PBS containing 10% normal goat serum and 0.05% Tween-20. A 1:4000 dilution of AlexaFluor 488-conjugated α-bungarotoxin was applied for 30 min at room temperature followed by three 5-min washes with PBS before mounting in ProLong Antifade Reagent.

Motor endplates were imaged on a Nikon PCM Confocal Microscope (Augusta, Georgia) using a 60X (1.4 NA) oil-immersion objective, and images were collected with SimplePCI software. The fluorochrome was excited with the 488-nm line of an argon laser and detected using a 515–530-nm band pass emission filter. Quantitative analysis of 8-bit, 640 × 480 pixel, TIFF images of endplates was performed using Scion Image for Windows (http://www.scioncorp.com) on samples acquired with identical laser power and gain settings (black level, 1024; PMT gain, 1593; scan time, 16 s). Endplates in the same focal plane from 3 $AChE^{+/+}$ mice (33 endplates) and 3 $AChE^{-/-}$ mice (42 endplates) were outlined using the freehand tool and analyzed for mean integrated pixel density and surface area. To compensate for differences in area between wild-type and AChE knockout mice, integrated density was divided by endplate area to yield normalized values of pixel density per μm^2.

Electron Microscopy. Muscles were fixed by immersion in buffered 1.6% paraformaldehyde/2.5% glutaraldehyde at 4°C. After 24 h of fixation, muscles were washed 3 times for 15 min each in 0.1M Na cacodylate buffer (pH 7.4, 194 mOsm/kg) and postfixed for 30 min in buffered 1% osmium tetroxide. Tissues were dehydrated through graded ethanol, followed by two 15-min washes in propylene oxide. Specimens were then incubated in propylene oxide and Poly/bed 812 at ratios of 1:1 and 1:3 for 2 h each, followed by incubation in pure resin overnight under vacuum. Tissues were flat embedded and polymerized at 60°C for 24 h. Semithin sections were used for preliminary morphological assessment and to select areas of interest for electron microscopy (EM). Ultrathin tissue sections were collected on copper mesh supporting grids, counterstained using uranyl acetate and lead citrate, and examined with a JEOL 1200EX transmission electron microscope (JEOL Inc., Peabody, Massachusetts).

Materials. AlexaFluor 488-conjugated α-bungarotoxin and ProLong Antifade Reagent were purchased from Molecular Probes (Eugene, Oregon). Acetylthiocholine iodide, butyrylthiocholine iodide, iso-OMPA, BW 248C51, dithiobisnitrobenzoic acid, Tween-20, OCT embedding medium, and all routine reagents were obtained from Sigma-Aldrich, St. Louis, Missouri. Poly/Bed 812 resin, propylene oxide, and sodium cacodylate were from Polysciences, Inc. (Warrington, Pennsylvania). Glutaraldehyde, paraformaldehyde and osmium tetroxide were from Electron Microscopy Sciences (Fort Washington, Pennsylvania). Ensure Fiber was from Ross Laboratories, Columbus, Ohio. Sylgard was obtained from Dow Corning (Midland, Michigan).

Data Analysis. Unless stated otherwise, data are expressed as the mean ± SEM. Statistical analysis was performed using Statistical Package for the Social Sciences (SPSS Inc., Chicago, Illinois). Comparisons between two groups were analyzed using a two-tailed Student's *t*-test, whereas comparisons between three or more groups were analyzed by an analysis of variance (ANOVA) followed by Bonferroni post hoc tests. For the data displayed in Figure 3, a two-factor ANOVA (frequency X treatment) was performed followed by one-way ANOVA and Bonferroni-planned comparisons to analyze significant interactions. A P value ≤ 0.05 was considered to be statistically significant.

RESULTS

Twitch Tensions in $AChE^{-/-}$ Muscle Have Enhanced Amplitude and Prolonged Time Course. Representative traces and summary data of indirectly elicited twitches from phrenic nerve–hemidiaphragm preparations of 8–21 $AChE^{+/+}$ and 9–11 $AChE^{-/-}$ mice are shown in Figure 1. Control diaphragms had peak twitch tensions of 0.9 ± 0.1g, rise times (10–90%) of 7.7 ± 0.5 ms and relaxation times (90–10%) of 17.4 ± 0.6 ms (Figs. 1A, 1E, and 1F). Twitch tensions from $AChE^{-/-}$ mice had markedly greater amplitudes (4.7 ± 0.4 g) and slower rise (15.9 ± 0.8 ms) and relaxation times (24.0 ± 0.9 ms) (Figs. 1B, 1E, and 1F).

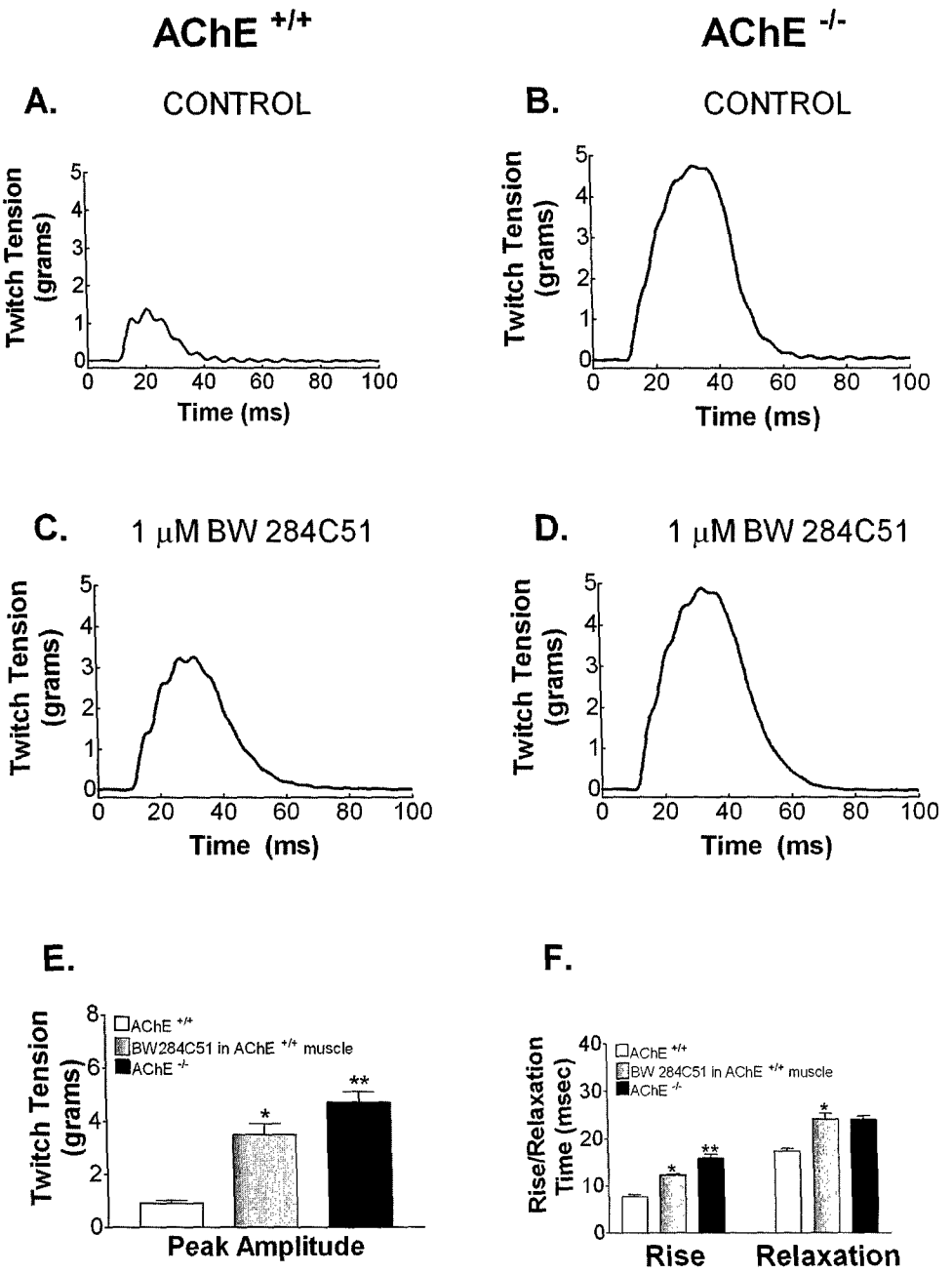

FIGURE 1. Single isometric twitch tensions in mouse hemidiaphragm muscle. The phrenic nerve was stimulated with 0.2-ms supramaximal voltages. Representative traces are shown in **A–D**, whereas pooled data are depicted in **E** and **F**. Conditions are as follows: **(A)** Twitch from an AChE$^{+/+}$ mouse. **(B)** Twitch from an age-matched AChE$^{-/-}$ mouse. **(C)** Muscle shown in **A** in the presence of 1 μM BW 284C51 to inhibit AChE selectively. **(D)** Muscle shown in **B** in the presence of 1 μM BW 284C51. **(E)** Histograms of peak twitch tension in wild-type and AChE$^{-/-}$ mice. Diaphragms were equilibrated for 20 min in 1 μM BW 284C51 prior to recording. **(F)** Histograms of rise and relaxation times of muscle twitches. A single asterisk represents significant differences between AChE$^{-/-}$ and AChE$^{+/+}$ muscles; double asterisks represent significant differences from both AChE$^{+/+}$ muscles and AChE$^{+/+}$ muscle treated with 1 μM BW 284C51. Data in **E** and **F** were obtained from 8–21 AChE$^{+/+}$ mice and 9–11 AChE$^{-/-}$ mice.

To determine whether the larger amplitudes and slower kinetics of muscle responses in AChE$^{-/-}$ mice were caused by accumulation of ACh, we examined tensions in wild-type mice after incubation with the selective AChE inhibitor BW 284C51. Addition of 1 μM BW 284C51, which depressed AChE activity by 97.8 ± 0.7% (n = 7), led to marked twitch potentiation in diaphragms of wild-type mice; peak tension was increased to 3.5 ± 0.4 g and the rise and relaxation times were prolonged to 12.4 ± 0.2 and 24.2 ±

1.2 ms, respectively (Figs. 1C, 1E, and 1F). Exposure to BW 284C51 did not potentiate twitch tension in $AChE^{-/-}$ mice (Fig. 1D), consistent with the absence of AChE in these animals.

Muscle from $AChE^{-/-}$ Mice Can Sustain Tetanic Tension at Intermediate Stimulation Frequencies. The ability of diaphragm muscles from $AChE^{-/-}$ mice to develop and maintain tetanic tension was probed by recording responses to repetitive stimulation of the phrenic nerve at frequencies ranging from 20 to 400 Hz. Muscles from wild-type mice maintained tension at these frequencies with little or no decrement (Fig. 2A). Diaphragms from $AChE^{-/-}$ mice were able to generate sustained tetanic responses at 70 and 100 Hz, but higher or lower stimulation frequencies led to progressive reductions in muscle tension (Fig. 2B).

To determine whether the tension profile exhibited by $AChE^{-/-}$ mice was consistent with a loss of AChE activity, hemidiaphragm preparations from $AChE^{+/+}$ mice were exposed to the selective AChE inhibitor, BW 284C51. In the presence of 1 μM BW 284C51, a frequency-dependent reduction of tension was observed in muscles from wild-type mice at all frequencies examined (Fig. 2C). In contrast, 1 μM BW 284C51 had no inhibitory effect on muscle contractility in $AChE^{-/-}$ hemidiaphragms. In fact, BW 284C51 improved muscle responses at 200 and 400 Hz (Fig. 2D), presumably by a direct postsynaptic action.[3,4] The lack of frequency-dependent inhibition by BW 284C51 in $AChE^{-/-}$ muscle is consistent with an absence of the target enzyme in the knockout mice.[13,36]

The fade in tetanic tension observed in diaphragm muscles from $AChE^{+/+}$ mice exposed to BW 284C51 was considerably more pronounced than that found in $AChE^{-/-}$ mice under any condition examined. This suggests that muscles from $AChE^{-/-}$ mice have adapted to function in an AChE-free environment. In principle, there are a number of possible mechanisms that can compensate for the absence of AChE. These include hydrolysis of ACh by BChE, reduction in nAChR density, remodeling of the endplate, reduction in ACh release, and alterations in the nAChR desensitization rate. The first three mechanisms are directly addressed in this study.

BChE Contributes to ACh Hydrolysis in $AChE^{-/-}$ Mice. To examine the possibility that BChE may be responsible for hydrolysis of transmitter in $AChE^{-/-}$ mice, muscle tension was elicited in the presence of iso-OMPA, a selective inhibitor of BChE.[4,11] Iso-OMPA (1 μM) had no effect on muscle tensions in $AChE^{+/+}$ diaphragms (Fig. 2E), although it inhibited BChE in these muscles by 75.1 $\pm$ 3.5% ($n = 7$). This lack of effect is consistent with the ability of wild-type muscles to hydrolyze transmitter by AChE, the dominant ChE at motor endplates.[11,33] In $AChE^{-/-}$ mice, 1 μM iso-OMPA produced a comparable inhibition of BChE activity (70.2 $\pm$ 2.9%, $n = 4$) and depressed muscle responses at frequencies $\geq$ 70 Hz (Fig. 2F). This suggests that BChE is responsible, at least in part, for the ability of diaphragms from $AChE^{-/-}$ mice to generate sustained tetanic tensions.

Diaphragm Muscles of $AChE^{-/-}$ Mice Have Reduced nAChR Density. A possible compensation for the absence of AChE activity in diaphragm muscles of $AChE^{-/-}$ mice is a reduction in nAChR density. This would have the effect of minimizing ACh persistence by favoring free diffusion of transmitter.[21,22,25] To determine whether reductions in receptor density could account for the ability of $AChE^{-/-}$ preparations to maintain tetanic tension, contractions were elicited in wild-type muscles exposed simultaneously to BW 284C51 to inhibit AChE and to *d*-tubocurarine (d-TC) to block nAChRs.[21,25] A d-TC concentration of 0.1 μM was selected because this results in marked nAChR blockade but avoids complications from direct channel effects that occur at higher d-TC concentrations.[9,35]

In $AChE^{+/+}$ muscle, 0.1 μM d-TC coapplied with 1 μM BW 284C51 partially antagonized the marked tetanic fade observed in the presence of BW 284C51 alone (Fig. 3A). The tension–frequency profile of wild-type muscles exposed to a combination of BW 284C51 and d-TC resembled that observed in control $AChE^{-/-}$ preparations (Fig. 3B). In $AChE^{-/-}$ mice, tetanic fade elicited at frequencies $\geq$ 200 Hz was antagonized by either 0.1 μM d-TC, 1 μM BW 284C51, or a combination of the two agents (Fig. 3B). This paradoxic enhancement of muscle tone may be produced by a direct action of BW 284C51, similar to that described in airway smooth muscle,[3,4] which is presumably obscured in wild-type preparations by the dominant effects of AChE inhibition.

Reduced nAChR Density Determined by Laser Confocal Microscopy. Direct evidence that endplates of $AChE^{-/-}$ mice have a lower receptor density was obtained by incubating muscles with the specific nAChR probe, α-bungarotoxin,[32] conjugated with the fluorescent dye AlexaFluor 488 (Figs. 4B and 4D). Analysis of normalized pixel intensity revealed a value of 1315 $\pm$ 44 pixels/μm^2 from 33 wild-type endplates and 711 $\pm$ 61 pixels/μm^2 from 42 AChE

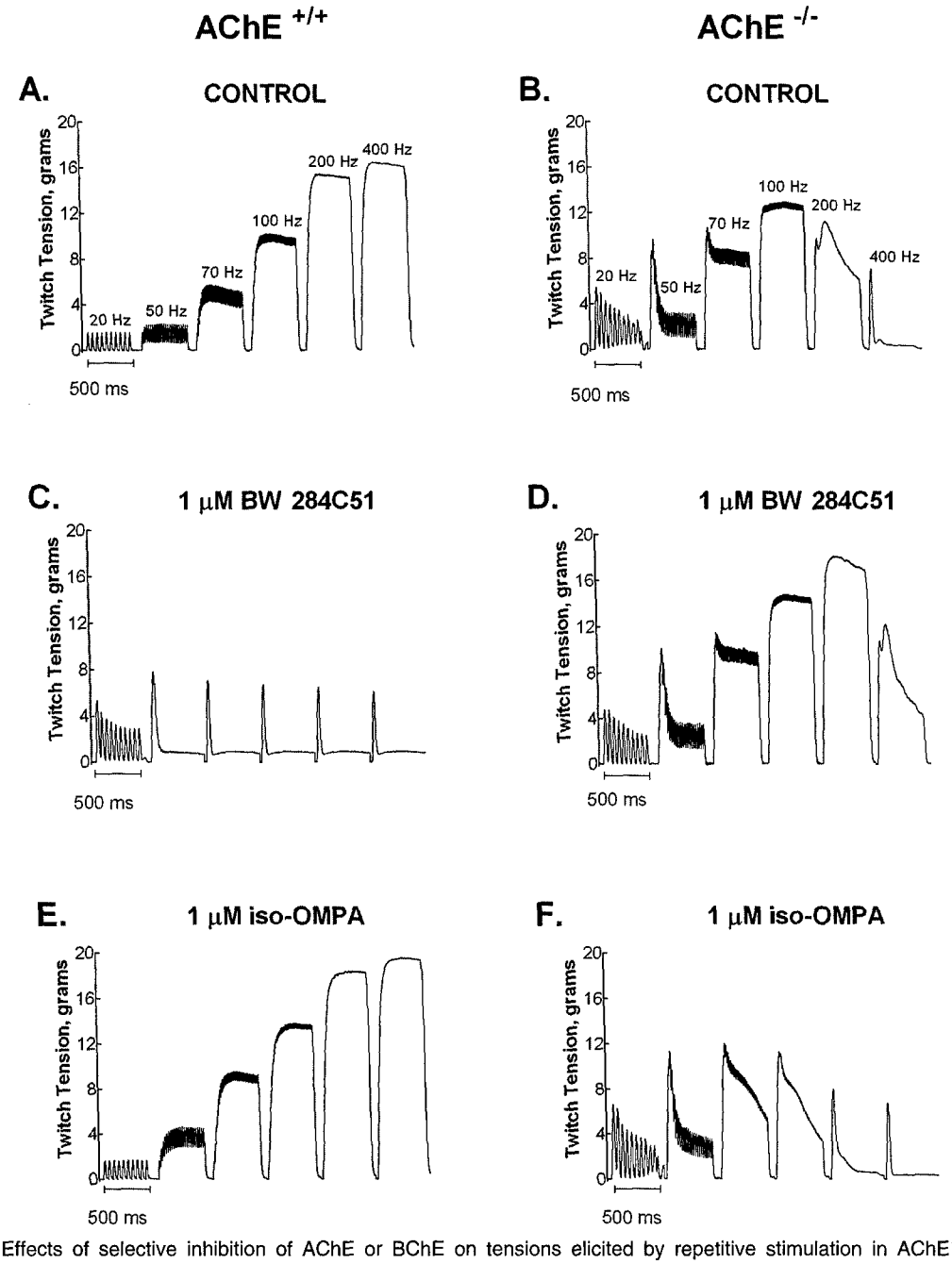

FIGURE 2. Effects of selective inhibition of AChE or BChE on tensions elicited by repetitive stimulation in $AChE^{+/+}$ and $AChE^{-/-}$ hemidiaphragms. Each panel shows tensions resulting from 500-ms trains of stimuli to the phrenic nerve at 20, 50, 70, 100, 200, and 400 Hz. The muscle was allowed to rest for 30 s between trains. **(A)** Tensions elicited from an $AChE^{+/+}$ hemidiaphragm. **(B)** Tensions elicited from an age-matched $AChE^{-/-}$ hemidiaphragm. **(C)** Muscle shown in A in the presence of 1 μM BW 284C51. **(D)** Muscle shown in B in the presence of 1 μM BW284C51. **(E)** Muscle shown in A after washout of BW 284C51 and addition of 1 μM iso-OMPA to inhibit BChE selectively. **(F)** Muscle shown in **B** after washout of BW 284C51 and addition of 1 μM iso-OMPA. Preparations were equilibrated for 20 min with each drug solution and washed for at least 30 min in physiological solution before addition of iso-OMPA.

knockout endplates, a 46% reduction ($P \leq 0.05$). The large difference in pixel intensity suggests that the $AChE^{-/-}$ mice have downregulated a large fraction of surface nAChRs to compensate for the chronic excess of ACh. This result is consistent with reductions of muscarinic ACh receptors (mAChRs) that have been found in brains of $AChE^{-/-}$ mice and in brains of normal mice exposed chronically to anti-ChE agents.[7,31,34]

In addition to differences in nAChR density, endplates from $AChE^{-/-}$ mice were also found to have a significantly smaller surface area, as revealed by Al-

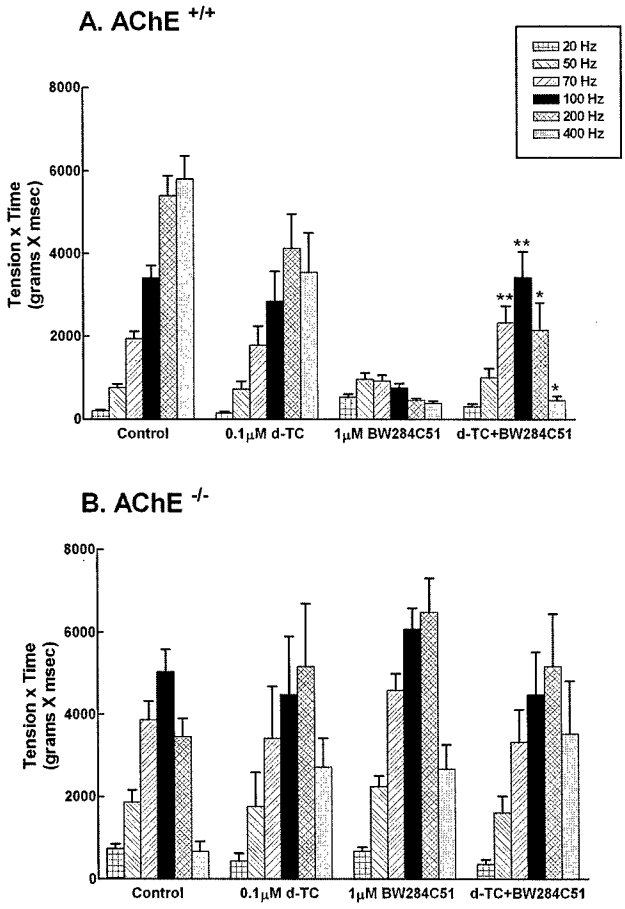

FIGURE 3. Tetanic tensions in $AChE^{+/+}$ and $AChE^{-/-}$ hemidiaphragms. Trains were elicited with 500-ms duration stimuli to the phrenic nerve at 20, 50, 70, 100, 200, and 400 Hz. The muscle was allowed to rest for 30 s between trains. Diaphragms were equilibrated for 20 min with each drug solution and washed with physiological solution for at least 30 min to remove d-TC prior to adding BW 284C51. **(A)** Responses from $AChE^{+/+}$ muscles under the indicated conditions. Note the marked tetanic fade in the presence of the AChE inhibitor BW 284C51 and the partial restoration of tension in the presence of BW 284C51 and d-TC at 70 and 100 Hz. The single asterisk represents a significant difference from control, whereas the double asterisk denotes significance from the BW284C51 group ($P \leq 0.05$; see Materials and Methods for details). **(B)** Responses from $AChE^{-/-}$ muscles under the indicated conditions. Note that both d-TC and BW 284C51 showed a trend toward enhancing tetanic tensions at the two highest frequencies. The bars represent the mean ± SEM of data obtained from four to six muscles.

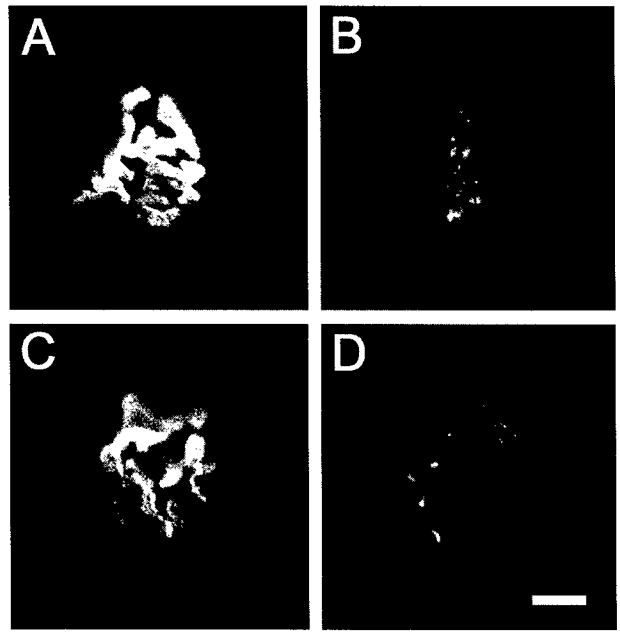

FIGURE 4. Fluorescent images of endplates from mouse hemidiaphragm muscles. Muscles were fixed, labeled with Alexa Fluor 488-α-bungarotoxin conjugate (1:4000 dilution) and examined by confocal microscopy. **(A and C)** Two representative wild-type ($AChE^{+/+}$) endplates. **(B and D)** Two representative AChE knockout endplates. Photomicrographs were obtained using the same parameters in order to perform quantitative analysis using Scion Image software. (Scale bar, 10 μm.)

exaFluor 488-conjugated α-bungarotoxin staining (Figs. 4B and 4D). Analysis of the images used for receptor density measurements disclosed a surface area of 432 ± 22 μm^2 for wild-type endplates and 247 ± 15 μm^2 for $AChE^{-/-}$ endplates, a decrease of 43% ($P \leq 0.05$).

Endplates Are Remodeled in $AChE^{-/-}$ Mice. An additional feature of $AChE^{-/-}$ diaphragm muscles was an alteration in endplate morphology. Unlike endplates from wild-type mice (Figs. 4A and 4C), those from the $AChE^{-/-}$ mice appear to be fragmented with multiple unstained regions interrupting areas of bright fluorescence (Figs. 4B and 4D). To exclude the possibility that darker areas of $AChE^{-/-}$ endplates were in a different focal plane, serial images were taken by confocal microscopy at 0.5 μm intervals through 10-μm–thick sections. Three-dimensional reconstructions of these endplates revealed a profile similar to those obtained from single optical sections, with a comparable pattern of discontinuities of fluorescence intensity (data not shown).

To shed light on the altered morphology observed by confocal microscopy, we examined endplates at a higher resolution using transmission EM. A typical neuromuscular junction from a control mouse and one from an age-matched $AChE^{-/-}$ animal are shown in Figure 5. Endplates from wild-type mice exhibited normal synaptic ultrastructure: nerve terminals contained abundant synaptic vesicles, and junctional folds were uniform and regular (Fig. 5A). In $AChE^{-/-}$ endplates, nerve terminals were fragmented: several smaller projections occupied a single postsynaptic site (Fig. 5B), leaving segments of

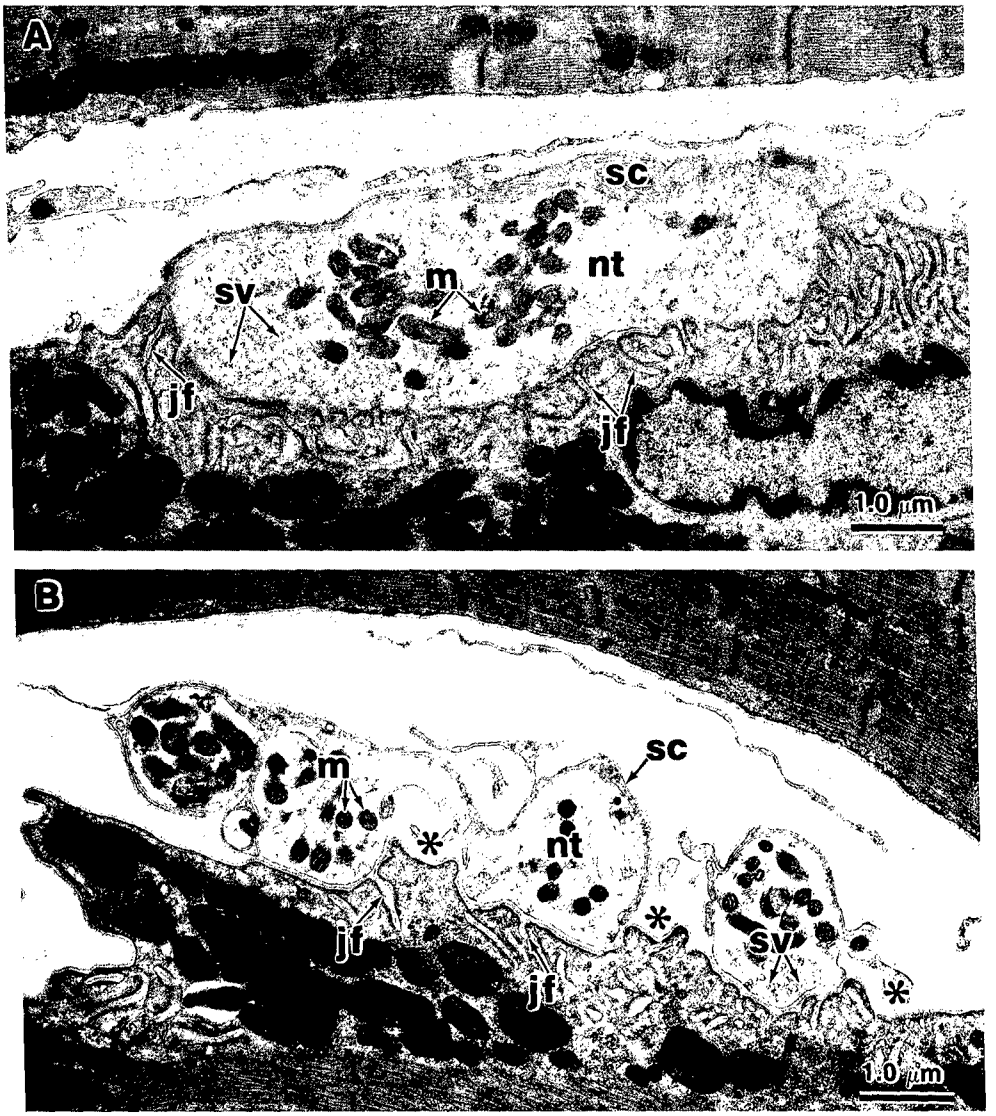

FIGURE 5. Electron micrographs of endplate regions from hemidiaphragms of AChE$^{+/+}$ and AChE$^{-/-}$ mice. **(A)** In endplates of AChE$^{+/+}$ mice, the nerve terminal (nt) has abundant mitochondria (m) and synaptic vesicles (sv) and is precisely aligned with postsynaptic junctional folds (jf). **(B)** The AChE$^{-/-}$ endplates exhibit marked alterations including fragmented nerve terminals, irregular junctional folds, and regions of postjunctional membrane lacking innervation (asterisks). In addition, Schwann cell (sc) processes have been observed to extend into the synaptic cleft. However, no generalized organelle damage was observed in AChE$^{-/-}$ endplates.

postjunctional membrane without effective innervation.

Junctional folds in AChE$^{-/-}$ muscle were shallow, irregular, and less numerous than those in wild-type endplates. The endplate of AChE$^{-/-}$ synapses appeared to be located on the surface of the muscle (Fig. 5B), rather than in synaptic troughs below the muscle surface, as seen in wild-type specimens (Fig. 5A). In addition, Schwann cell processes were often extended into the synaptic cleft. However, focal swelling of mitochondria or of endoplasmic reticular membranes, which are features of acute inhibition of AChE,[23] were not observed in AChE knockout endplates.

DISCUSSION

The AChE$^{-/-}$ mice were smaller than their age-matched littermates and exhibited an unsteady gait, muscle weakness, tremors, and a high susceptibility to seizures.[7,14] Despite these abnormalities, the ability of these mice to survive in the absence of the critical enzyme AChE is remarkable and suggests that the cholinergic system is capable of extensive compensation involving both the central and peripheral systems.

We examined the characteristics of nerve evoked contraction in diaphragm muscle from AChE$^{-/-}$ mice. As revealed by the records of Figure 1, single-

twitch tensions were markedly augmented in both amplitude and time course, and tensions elicited by repetitive stimulation were well maintained at 70 and 100 Hz but not at higher or lower frequencies (Fig. 2). The latter finding indicates partial adaptation to excess ACh.

Augmentation of single twitches in knockout mice can be attributed to inhibition of AChE, because twitch potentiation is a well-documented consequence of ACh accumulation.[19] This conclusion is further supported by the finding that exposure of diaphragm muscle from wild-type mice to the selective AChE inhibitor BW 284C51 produced single twitches with increased amplitudes and prolonged rise and relaxation times similar to those observed in $AChE^{-/-}$ muscle. The slightly greater twitch potentiation observed in the AChE knockout mice (Fig. 1B) compared with the acutely inhibited wild-type muscle (Fig. 1C) can be explained by the incomplete block of AChE by BW 284C51.

Twitch potentiation is considered to arise from multiple muscle action potentials following a single stimulus, which may be triggered by repetitive nerve impulses (backfiring) or from a single prolonged endplate potential.[8,25] The latter would appear to be excluded because prolonged endplate potentials, sufficient to trigger multiple action potentials, were not observed in preliminary electrophysiological studies (unpublished observations; see Minic et al.[26]). The finding that $AChE^{-/-}$ mice exhibited twitch potentiation similar to that of muscles in which AChE was acutely inhibited suggests that this phenomenon does not undergo adaptation.

The tension–frequency profiles observed during repetitive stimulation in $AChE^{-/-}$ mice were intermediate between the decremental responses that follow acute inhibition of AChE activity and the sustained responses of normal muscle (Fig. 2). In AChE-inhibited muscle, reductions in tension during repetitive stimulation reflect an underlying desensitization of nAChRs following accumulation of ACh.[12,17] Desensitization is suggested by the decrease in the amplitude of successive responses at 20 Hz and by tetanic fade at 200 Hz and 400 Hz (Fig. 2B). The sustained tensions observed at 70 Hz and 100 Hz in $AChE^{-/-}$ muscle would then represent a balance between desensitization of nAChRs and the normal process of tetanic summation. Although not apparent, desensitization in $AChE^{-/-}$ diaphragms may also be occurring at 70 Hz and 100 Hz, as indicated by reduction in the tetanus to twitch ratio. At 100 Hz, this ratio was 7.5 in $AChE^{+/+}$ mice (Figs. 1A and 2A) but only 2.2 in $AChE^{-/-}$ mice (Figs. 1B and 2B). The finding that diaphragm muscles from $AChE^{-/-}$ mice can maintain tension during repetitive stimulation, albeit over a limited frequency range, suggests that ACh accumulation or its consequences undergo compensatory changes to maintain function.

The first of three possible mechanisms examined in this study for partial compensation of tetanic fade in $AChE^{-/-}$ mice was hydrolysis of ACh by BChE. This enzyme is not generally thought to contribute to removal of ACh but can do so when AChE is inhibited.[3,4] In $AChE^{-/-}$ mice, BChE activity was reported to be comparable to that found in $AChE^{+/+}$ mice with a similar distribution.[7,24,26] Although no compensatory increase in BChE activity occurs in AChE knockout mice, this enzyme appears to exert a prominent role in maintaining muscle function, as indicated by the enhanced tetanic fade observed in the presence of 1 μM iso-OMPA at frequencies $\geq$70 Hz (Fig. 2F). In wild-type mice, where AChE is fully active, 1 μM iso-OMPA has no discernible effect on tetanic tension (Fig. 2E). A similar role for BChE was suggested by Chatonnet et al.,[7] based on their results with the selective BChE inhibitor, bambuterol.

A second possible mechanism for maintenance of tetanic tension in $AChE^{-/-}$ mice is downregulation of nAChRs. Data from fluorescent α-bungarotoxin studies revealed a 46% reduction in receptor density in $AChE^{-/-}$ mice. This reduction may actually be underestimated, due to the fact that the scan time needed to observe endplates from knockout mice resulted in image saturation for some wild-type specimens. The decrease in nAChR density is suggested to result from functional downregulation of nAChRs, mediated perhaps by increased receptor internalization in response to excess ACh in the synaptic cleft. This finding is consistent with a recent study reporting reduced surface levels and enhanced intracellular disposition of mAChRs from $AChE^{-/-}$ mice.[34] Downregulation of both nAChRs and mAChRs was reported by Chatonnet et al.,[7] who found reduced sensitivity to nicotine and muscarine in isolated brainstem preparations of $AChE^{-/-}$ mice.

Inhibition of AChE activity results in repeated binding of ACh to nAChRs, a key factor responsible for the persistence of ACh at the neuromuscular junction.[21] A lower receptor density allows efflux of ACh to approach free diffusion conditions, leading to less severe desensitization and thus to less pronounced tetanic fade.[21,25] Evidence for the role of nAChR downregulation in the maintenance of muscle function was provided by findings that BW 284C51–induced tetanic fade in wild-type mice was antagonized by addition of 0.1 μM d-TC (Fig. 3A), a concentration that corresponds to approximately 2.5 times the IC_{50} for nAChR inhibition.[35] Reductions in

nAChR density comparable to those found in the current study have been observed in muscles from patients with a congenital deficiency of collagen-tailed AChE.[20]

The third mechanism examined was synaptic remodeling. Confocal microscopic examination of endplates from AChE$^{-/-}$ mice revealed a smaller surface area and discontinuities in α-bungarotoxin fluorescence, suggesting an altered pattern of nAChR distribution (Fig. 4). The pattern resembled that found in newly formed endplates of muscle fibers that were innervated de novo in a region outside existing endplates.[18] This similarity suggests that the knockout endplates revert to an immature state prevalent early in development to compensate for the presence of excess ACh.

Significant changes in neuromuscular junction morphology were also evident at the ultrastructural level (Fig. 5). In AChE$^{-/-}$ mice, junctional folds were fewer in number, irregular, and shallow. In many of these junctions, the nerve terminal appeared to be fragmented, with several smaller terminals occupying a single endplate. Such terminals formed synapses with only a portion of the postsynaptic region, leaving the remainder without effective innervation (Fig. 5B). These morphological changes resemble those of patients with congenital myasthenic syndromes caused by the absence of collagen-tailed AChE at motor endplates.[16,20] The cumulative effect of synaptic remodeling may be to reduce the presynaptic and postsynaptic contacts and to open additional pathways for diffusion of ACh. For example, the reduced nAChR density coupled with the fragmented nerve terminals would facilitate the escape of ACh from the synaptic cleft, because ACh would have multiple diffusion pathways and fewer binding sites to hinder its removal from the synaptic cleft. This increased rate of diffusion of ACh may account, in part, for the finding that tetanic tensions in AChE knockout mice are better maintained than expected (Figs. 2 and 3).

In addition to the three mechanisms examined, other factors may also be involved in preservation of function in AChE$^{-/-}$ mice: these include changes in the rate of nAChR desensitization and reductions in quantal content and in quantal size. The contribution of these factors will be examined in future studies.

One of the authors (H. A. M.) is a National Research Council (NRC) post-doctoral fellow.

REFERENCES

1. Aas P, Veitberg T, Fonnum F. In vitro effects of soman on bronchial smooth muscle. Biochem Pharmacol 1986;35:1793-1799.
2. Adler M, Moore DH, Filbert MG. Mechanism of soman-induced contractions in canine tracheal smooth muscle. Arch Toxicol 1992;66:204-210.
3. Adler M, Petrali JP, Moore DH, Filbert MG. Function and distribution of acetyl- and butyrylcholinesterase in canine tracheal smooth muscle. Arch Int Pharmacodyn Ther 1991; 312:126-139.
4. Adler M, Reutter SA, Moore DH, Filbert MG. Regulation of acetylcholine hydrolysis in canine tracheal smooth muscle. Eur J Pharmacol 1991;205:73-79.
5. Ceccarelli B, Hurlbut WP, Mauro A. Turnover of transmitter and synaptic vesicles at the frog neuromuscular junction. J Cell Biol 1973;57:499-524.
6. Chang FC, Foster RE, Beers ET, Rickett DL, Filbert MG. Neurophysiological concomitants of soman-induced respiratory depression in awake, behaving guinea pigs. Toxicol Appl Pharmacol 1990;102:233-250.
7. Chatonnet F, Boudinot E, Chatonnet A, Taysse L, Daulon S, Champagnat J, Foutz AS. Respiratory survival mechanisms in acetylcholinesterase knockout mouse. Eur J Neurosci 2003; 18:1419-1427.
8. Clark AL, Hobbiger F, Terrar DA. Nature of the anticholinesterase-induced repetitive response of rat and mouse striated muscle to single nerve stimuli. J Physiol (Lond) 1984;349:157-166.
9. Colquhoun D, Dreyer F, Sheridan RE. The actions of tubocurarine at the frog neuromuscular junction. J Physiol (Lond) 1979;293:247-284.
10. Couteaux R. Remarks on the organization of axon terminals in relation to secretory processes at synapses. Adv Cytopharmacol 1974;2:369-379.
11. Davis R, Koelle GB. Electron microscopic localization of acetylcholinesterase and nonspecific cholinesterase at the neuromuscular junction by the gold-thiocholine and gold-thiolacetic acid methods. J Cell Biol 1967;34:157-171.
12. Dudel J, Heckmann M. Desensitization reduces amplitudes of quantal end-plate currents after a single preceding end-plate current in mouse muscle. Pflugers Arch 1999;437:569-576.
13. Duysen EG, Li B, Xie W, Schopfer LM, Anderson RS, Broomfield CA, Lockridge O. Evidence for nonacetylcholinesterase targets of organophosphorus nerve agent: supersensitivity of acetylcholinesterase knockout mouse to VX lethality. J Pharmacol Exp Thera 2001;299:528-535.
14. Duysen EG, Stribley JA, Fry DL, Hinrichs SH, Lockridge O. Rescue of the acetylcholinesterase knockout mouse by feeding a liquid diet; phenotype of the adult acetylcholinesterase deficient mouse. Dev Brain Res 2002;137:43-54.
15. Ellman GL, Courtney KD, Andres V, Featherstone RM. A new rapid colorimetric determination of acetylcholinesterase activity. Biochem Pharmacol 1961;7:88-95.
16. Engel AG, Lambert EH, Mulder DM, Torres CF, Sahashi K, Bertorini TE, Whitaker JN. A newly recognized congenital myasthenic syndrome attributed to a prolonged open time of the acetylcholine-induced ion channel. Ann Neurol 1982;11: 553-569.
17. Giniatullin RA, Magazanik LG. Desensitization of the postsynaptic membrane of neuromuscular synapses induced by spontaneous quantum secretion of mediator. Neurosci Behav Physiol 1998;28:438-442.
18. Gwyn DG, Aitken JT. The formation of new motor endplates in mammalian skeletal muscle. J Anat 1966;100(1):111-126.
19. Heffron PF, Hobbiger F. Relationship between inhibition of acetylcholinesterase and response of the rat phrenic nerve-diaphragm preparation to indirect stimulation at higher frequencies. Br J Pharmacol 1979;66:323-329.
20. Hutchinson DO, Walls TJ, Nakano S, Camp S, Taylor P, Harper CM, Groover RV, Peterson HA, Jamieson DG, Engel AG. Congenital endplate acetylcholinesterase deficiency. Brain 1993;116:633-653.
21. Katz B, Miledi R. The binding of acetylcholine to receptors and its removal from the synaptic cleft. J Physiol (Lond) 1973;231:549-574.

22. Land BR, Salpeter EE, Salpeter MM. Kinetic parameters for acetylcholine interaction in intact neuromuscular junction. Proc Natl Acad Sci (USA) 1981;78:7200-7204.
23. Laskowski MB, Olson WH, Dettbarn WD. Initial ultrastructural abnormalities at the motor end plate produced by a cholinesterase inhibitor. Exp Neurol 1977;57(1):13-33.
24. Li B, Stribley JA, Ticu A, Xie W, Schopfer LM, Hammond P, Brimijoin S, Hinrichs SH, Lockridge O. Abundant tissue butyrylcholinesterase and its possible function in the acetylcholinesterase knockout mouse. J Neurochem 2000;75:1320-1331.
25. Magleby KL, Terrar DA. Factors affecting the time course of decay of end-plate currents: a possible cooperative action of acetylcholine on receptors at the frog neuromuscular junction. J Physiol (Lond) 1975;244:467-495.
26. Minic J, Chatonnet A, Krejci E, Molgo J. Butyrylcholinesterase and acetylcholinestrase activity and quantal transmitter release at normal and acetylcholinesterase knockout mouse neuromuscular junctions. Br J Pharmacol 2003;138:177-187.
27. Neher E, Sakman B. Single channel currents recorded from membrane of denervated frog muscle fibres. Nature 1976; 260:799-802.
28. Okudera H. Clinical features on nerve gas terrorism in Matsumoto. J Clin Neurosci 2002;9:17-21.
29. Rickett DL, Glenn JF, Beers ET. Central respiratory effects versus neuromuscular actions of nerve agents. Neurotoxicol 1986;7:225-236.
30. Rosenberry TL. Quantitative simulation of endplate currents at neuromuscular junctions based on the reaction of acetylcholine with acetylcholine receptor and acetylcholinesterase. Biophys J 1979;26:263-289.
31. Schlador ML, Grubbs RD, Nathanson NM. Multiple topological domains mediate subtype-specific internalization of the M2 muscarinic acetylcholine receptor. J Biol Chem 2000;275: 23295-23302.
32. Tzartos SJ, Changeux JP. High affinity binding of alpha-bungarotoxin to the purified alpha-subunit and to its 27,000-dalton proteolytic peptide from Torpedo marmorata acetylcholine receptor. EMBO J 1983;2:381-387.
33. Vigny M, Gisiger V, Massoulie J. "Nonspecific" cholinesterase and acetylcholinesterase in rat tissues: molecular forms, structural and catalytic properties, and significance of the two enzyme systems. Proc Natl Acad Sci (USA) 1978;75:2588-2592.
34. Volpicelli-Daley LA, Hrabovska A, Duysen EG, Ferguson SM, Blakely RD, Lockridge O, Levey AI. Altered striatal function and muscarinic cholinergic receptors in acetylcholinesterase knockout mice. Mol Pharmacol 2003;64(6):1309-1316.
35. Wenningmann I, Dilger JP. The kinetics of inhibition of nicotinic acetylcholine receptors by (+)-tubocurarine and pancuronium. Mol Pharmacol 2001;60:790-796.
36. Xie W, Stribley JA, Chatonnet A, Wilder PJ, Rizzino A, McComb RD, Taylor P, Hinrichs SH, Lockridge O. Postnatal developmental delay and supersensitivity to organophosphate in gene-targeted mice lacking acetylcholinesterase. J Pharmacol Exp Thera 2000;293:896-902.